Registration of Low-SNR, High-Resolution Diffusion-Weighted Images

S.F. Johnsen[1]
stian.johnsen.09@ucl.ac.uk
C.A. Clark[2]
cclark@ich.ucl.ac.uk
D. Atkinson[1]
d.atkinson@cs.ucl.ac.uk

[1] Centre for Medical Image Computing
University College London
London, UK

[2] Institute of Child Health
University College London
London, UK

Abstract

This paper introduces a novel, high-speed scheme for intrasubject registration and segmentation of high-resolution multi-shot diffusion-weighted images. Compared to single-shot sequences, multi-shot have advantages in terms of improved spatial resolution and reduced eddy-current and susceptibility artifacts. However, these sequences have prolonged scan times increasing the risk of subject motion, and, a lower signal to noise ratio (SNR) with smaller voxel volumes. The proposed registration algorithm comprises a hybrid thresholding expectation-maximization segmentation method that can cope with the low-SNR, and registers diffusion-weighted to B0 images through fast detection and matching of features found in edge images derived from floating and reference images. We performed validations of the entire pipeline, including assessment of visual appearance by experts, consistency error computations, and analysis of the segmentation, using volunteer images, and found its performance to be comparable with, or exceeding, that of established solutions.

1 Introduction

High-resolution multi-shot echo planar imaging (MS-EPI) sequences have advantages over single-shot EPI (SS-EPI) acquisitions in the visualization of small anatomical structures such as the internal features of the hippocampus. Further, they are less prone to susceptibility artifacts and eddy-current distortions. A significant problem with these high-resolution sequences, however, is the acquisition time. For instance, the readout-segmented EPI [2] sequence used for acquisition of our test data is roughly 11 times slower than SS-EPI. Even if only one series of images is to be acquired and the subject is healthy, keeping still for such a long time is difficult, but since high-resolution sequences also suffer from very low SNR, multiple series are typically acquired for improving the image quality by averaging which leads to additional misalignment problems.

As multi-shot sequences are still considered experimental, most of the work done on registration of diffusion-weighted images only addresses the distortions arising

from eddy currents which are dominant in SS-EPI images, with many of the existing post-processing techniques being derived from the iterative cross-correlation method [6]. Hence, the most widely used approach is to employ general-purpose multi-modal affine registration algorithms, usually based on mutual information (MI) [4] or correlation ratio (CR) [3].

2 Methods

Our proposed new registration algorithm essentially registers DW images to a B0 reference image, this is achieved with a feature-based, iterative affine registration scheme that operates on edge-images derived from floating and reference images. Since the main registration step uses features located on the outline of the brain, having a clean outline without cerebrospinal fluid (CSF) or scalp is very important. The pipeline therefore comprises a specialized segmentation method. Given an input of multiple image series, the output of the algorithm is one average B0 image, and for each diffusion-sensitizing gradient direction, one average DW image.
The registration pipeline can summarized by: Preregistration, segmentation, and DW to B0 registration based on edge-images.

2.1 Preregistration and Generation of Target B0 Image

The preregistration step registers B0 images of subsequent series to that of the first series. This serves two purposes: creation of the average B0 image and reduction of interseries subject-motion misalignment in DW images. Interseries movement is more likely, than that within a series, hence the transforms found for aligning the series' B0 images with the reference, ought to be capable correcting for the bulk of interseries misalignment between DW images, as well.

Feature-extraction: The B0 image features are extracted from a cornerness map which is given by the lower eigenvalue of per-pixel Harris matrices [1]. After the cornerness map is computed, the top 10% cornerness values are considered feature candidates which are further filtered by non-maximal suppression. Edge-suppression is not performed.

The registration process is iterative. Each loop iteration begins with the locating of a corresponding feature in the reference image for every floating image feature $\boldsymbol{x_f}$. This is done by exhaustively searching a window in the reference image centered at $\boldsymbol{x_f}$ for a location $\boldsymbol{x_r}$ that minimizes

$$f_c = \underbrace{\|\boldsymbol{n_F}(\boldsymbol{x_f}) - \boldsymbol{n_R}(\boldsymbol{x_r})\|^2}_{\text{Square difference of intensities}} + \underbrace{\|\boldsymbol{x_f} - \boldsymbol{x_r}\|^2}_{\text{Distance penalty}} \tag{1}$$

$\boldsymbol{n_F}(\boldsymbol{x_f})$ and $\boldsymbol{n_R}(\boldsymbol{x_r})$ are neighborhoods that cover about 3% of the floating and reference image, respectively.
Given these two sets of control points the optimal transform increment is computed with linear least-squares. The increment is subsequently, by right multiplication, incorporated into the global transform matrix.

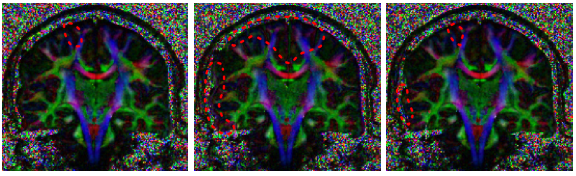

(a) Registration result: Artifacts are highlighted with red dotted lines. From left to right: Edge-image algorithm, FSL NMI, FSL CR.

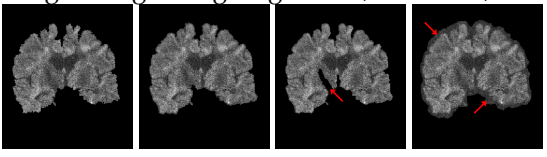

(b) Segmentation result: Artifacts are highlighted with red arrows. From left to right: Manual, EM/Thresholding, Act. contour, FSL BET.

Figure 1: Result images (best viewed electronically).

The algorithm stops when the relative difference between the accumulated transforms of two subsequent iterations drops below a threshold.

2.2 Segmentation

The segmentation algorithm comprises two major steps, initial segmentation by means of automatic thresholding and subsequent refinement by iterative application of an expectation-maximization (EM) code.

Thresholding: Finding a threshold for the DW images can be achieved with a smoothed histogram by setting the threshold between the first and second count maxima. Using the DW-image segmentation masks, the B0 image is segmented with a threshold bracket such that the overlap of the B0 segmentation mask and the union of the DW segmentation masks is maximal.

Expectation-Maximization Segmentation: Next, priors for a 4-class EM segmentation are computed. The prior for the white and gray matter areas is obtained by averaging all segmented DW images, and blurring and normalizing the average image. Initial priors for other anatomical-structure areas (scalp, and the like) and CSF are obtained by applying an inverted brain segmentation mask to the average B0 image and identifying suitable thresholds in a histogram of the segmented image. The segments obtained in this way are then blurred and normalized. The last prior, for background areas, is obtained by pixel-wise subtracting the maximum of the first three priors from a flat, all-one image.

Once 4-class EM segmentations of the B0 image are obtained, to improve on the initial CSF and "other structure" priors, gradually more weight is assigned to the masks returned by the EM algorithm. The algorithm typically stops after 4-5 iterations.

2.3 DW to B0 Registration

Extracting edge-images: A hysteresis edge detection algorithm [6] is applied with the aim of obtaining edges at the same anatomical locations in the segmented DW

Edge-Image	FSL NMI	FSL CR
(0.33, **1.26**, 0.56)	(0.04, 0.85, 0.4)	(**0.41**, **1.26**, **0.7**)

(a) Table of avg. expert scores. Format: (scorer 1, scorer 2, scorer 3).

Edge-Image	FSL NMI	FSL CR
(**1.44**, 3.29)	(3.74, 4.76)	(1.99, 2.74)

(b) Average consistency errors and displacements (in pixel units). In (const. error, displacement) format.

Table 1: Registration quality scores (best scores are in **bold**.)

images and B0 images. These are very strong edges that can be found on the outline of the brain, and also at interfaces between actual brain tissue and CSF. The high threshold image is determined such that 5% of the corresponding brain segmentation mask is covered with edges, the low threshold chosen such that 20% of the mask is covered.

The feature detection scheme places feature candidates at positions on the outline of a segmentation mask where the boundary curvature is locally maximal. These candidates are subsequently filtered with non-maximal suppression which yields sensible features over the entire length of the segmentation mask boundary.

Feature-matching and warping is done with the methods described in section 2.1.

3 Experiments and Results

The experiments were carried out on five volunteer image sets. All of these sets consisted of 4-6 series each of which in turn consisted of 6 DWIs and the usual B0 image. There was varying amounts of subject motion in the test data, two sets had almost none or only little, 3 were severely misaligned.
The image data was acquired with the sequence described in [2] on a 1.5T Siemens scanner, the diffusion-weighting was 1000s/mm^2. The images had a matrix size of 256×192, and voxel dimensions of $0.9 \times 0.9 \times 5$mm with a 1mm slice gap.

Some typical registration results are displayed in figure 1(a) as color-coded fractional anisotropy (CFA) maps. 1(b) shows example segmentation results.

For **evaluating the segmentation pipeline**, results on a number of DW images from our algorithm, "Active contour without edges" [8], Brain Extraction Tool (BET) of FSL 4.1 (`http://www.fmrib.ox.ac.uk/fsl`), and manual segmentation were mutually compared with Dice's set similarity measure. In these experiments, it was apparent that the results from our EM-threshold hybrid algorithm, manual segmentation, and active contour are roughly the same, with Dice scores between 97% and 99%. In some cases though, such as the darker areas of the brain in figure 1(b), the low SNR and the anisotropy of the tissue led to areas of the brain being wrongly excluded from the mask by "Active contour with edges". FSL BET performed poorly with less than 90% agreement with the other methods.

The **evaluation of the full pipeline**, consisted of comparisons of FSL affine registration (FLIRT) with normalized MI (FSL NMI), and CR (FSL CR) cost functions with our proposed method by means of expert scoring of the visual quality of fractional anisotropy (FA) maps and CFA maps, and measuring algorithm robustness through consistency errors [7]. The images were scored in randomized order with the scorer blinded to the method. The scores were assigned on a per-slice basis ranging from -2 (unusable) to +2 (excellent). The average (over all 5 series) expert scores and consistency errors can be found in tables 1(a) and 1(b), respectively.
In terms of registration speed, the difference between our proposed method and FSL CR was negliglible with an average 431.04s and 430.5s, respectively, for registration of a full set. FSL NMI took on average 659.8s.

4 Discussion and Conclusions

Even with the method still being very experimental, the low consistency error, the quality of the output images, and also the timings, show that its performance is competitive with established solutions, and clearly exceeds that of FSL with the normalized mutual information cost function on this data. We also have shown, that our scheme does not only provide high-quality registration, but also a reliable and fast segmentation of these noisy high-resolution DW-MR images. So, we hope that this work will motivate and provide building blocks for new, specialized image registration methods for a type of diffusion-weighted imaging that holds a lot of promise for the study of the detailed structure of the brain in both health and disease.

References

[1] Harris C and Stephens M. A combined corner and edge detector. *Proc. Fourth Alvey Vision Conference*, pages 147–151, 1988.

[2] Porter DA and Heidemann RM. High resolution diffusion-weighted imaging using readout-segmented echo-planar imaging, parallel imaging and a two-dimensional navigator-based reacquisition. *Magnetic Resonance in Medicine*, 62:468–475, 2009.

[3] Roche A et al. The correlation ratio as a new similarity measure for multimodal image registration. *LNCS*, 1496:1115–1124, 1998.

[4] Maes F, Vandermeulen D, and Suetens P. Medical image registration using mutual information. *Proceedings of the IEEE*, 91:1699–1722, 2003.

[5] Canny J. A computational approach to edge detection. *IEEE Trans. Pattern Analysis and Machine Intelligence*, 8:679–698, 1986.

[6] Haselgrove JC and Moore JR. Correction for distortion of echo-planar images used to calculate the apparent diffusion coefficient. *MRM*, 36:960–964, 1996.

[7] Netsch T and van Muiswinkel A. Quantitative evaluation of image-based distortion correction in diffusion tensor imaging. *IEEE Trans. Medical Imaging*, pages 789–798, 2004.

[8] Chan TF and Vese LA. Active contours without edges. *IEEE Transactions on Image Processing*, 10: 266–277, 2001.